Global Coevolution of Human MicroRNAs and Their Target Genes

Shahar Barbash,*[,1] Sagiv Shifman,[2] and Hermona Soreq*[,1]

[1]Department of Biological Chemistry, The Institute of Life Sciences and The Edmond & Lily Safra Center for Brain Sciences, Hebrew University of Jerusalem, Jerusalem, Israel

[2]Department of Genetics, The Institute of Life Sciences, Hebrew University of Jerusalem, Jerusalem, Israel

***Corresponding author:** E-mail: hermona.soreq@mail.huji.ac.il; barbashshahar@gmail.com.

Associate editor: Joshua Akey

Abstract

MicroRNAs (miRNAs) have presumably contributed to the emergence of the novel expression patterns, higher brain functions, and skills underlying human evolution. However, it is incompletely understood how new miRNAs have evolved in the human lineage because their initial emergence predictably entailed deleterious consequences due to their powerful multitarget effects. Here, we report genetic variation and conservation parameters for miRNAs and their predicted targets in the genomes of 1,092 humans and 58 additional organisms. We show that miRNAs were evolutionarily more conserved than their predicted binding sites, which were inversely subject to the accumulation of single-nucleotide variations over short evolutionary timescales. Moreover, the predictably "younger" human-specific miRNAs presented lower genetic variation than other miRNAs; their targets displayed higher genetic variation compared with other miRNA targets in diverse human populations; and neuronal miRNAs showed yet lower levels of genetic variation and were found to target more protein-coding genes than nonneuronal miRNAs. Furthermore, enrichment analysis indicated that targets of human-specific miRNAs primarily perform neuronal functions. Specifically, the genomic regions harboring the vertebrate-conserved neuronal miRNA-132 presented considerably higher conservation scores than those of its target genes throughout evolution, whereas both the recently evolved human miRNA-941 and its acquired targets showed relatively low conservation. Our findings demonstrate inversely correlated genetic variation around miRNAs and their targets, consistent with theories of coevolution of these elements and the predicted role attributed to miRNAs in recent human evolution.

Key words: **miRNA, coevolution, human evolution, brain.**

Introduction

Specific phenotypes that separate humans from other primates, such as language and tool making, are thought to have emerged due to massive differences in gene expression (Khaitovich et al. 2006). It has been suggested that evolution of complex gene-regulating networks enabled major changes in brain development (Oldham et al. 2006; Babbitt et al. 2010; Konopka et al. 2012). Specifically, the rapid speciation of humans compared with their closest living primates the chimpanzees was initially presumed to involve mutations in regulatory genome components that widely affect gene expression (King and Wilson 1975; Hu et al. 2011) such as transcription factors (Nowick et al. 2009). Recent studies address the role in this process of microRNAs (miRNAs), which are known to coregulate multiple targets involved in particular functional pathways (He and Hannon 2004; Lu et al. 2008; Fineberg et al. 2009). The short, single-stranded miRNA molecules regulate mRNA levels posttranscriptionally (Ambros 2003) by inducing their degradation (Bagga et al. 2005) and/or translational repression (Olsen and Ambros 1999). Single miRNAs may target several tens of genes (Stark et al. 2003), and a single gene can be regulated by several different miRNAs (Enright et al. 2003). Therefore, miRNAs are natural candidates for initiating the evolutionary rewiring of the human brain's regulatory networks. Furthermore, the small size of miRNAs predicts faster creation of new ones compared with protein-coding genes (Chen and Rajewsky 2007). Additionally, changes in the expression patterns of an existing miRNA may affect new sets of targets, forming novel regulatory circuits and changing pre-existing ones. Based on such arguments, and on miRNA expression patterns in different tissues and species, Khaitovich et al. postulated miRNA contributions to the accelerated evolution of the brain's transcriptome (Khaitovich et al. 2006; Somel et al. 2011). These and other studies further predicted and validated coevolution events for specific miRNAs and their targets in *Drosophila* (Tang et al. 2010) and for miRNA-941 in primate evolution (Hu et al. 2012). However, the nature of miRNA regulation and its genomic scope remained incompletely understood because these predictions of coevolution were limited to a few miRNAs and their target sites but have not yet been addressed in a global manner based on the human genome.

A previously proposed model for the evolutionary emergence of miRNAs suggests that new miRNAs are initially expressed at low levels, thus avoiding deleterious consequences and allowing the introduction of such new miRNAs into cellular circuits (Chen and Rajewsky 2007; Liang and Li 2009; Berezikov 2011; Roux et al. 2012). The next transitional

Article

phase involves mutation-driven elimination of deleterious miRNA sites, while maintaining or creating beneficial binding sites, which provide a selective advantage. Finally, the expression level of the established miRNAs can gradually increase, and small changes in the miRNA sequences and their binding sites lead to further refinement.

In this study, we aimed to explore these global evolutionary changes in miRNA genes and their binding sites. We specifically focused our tests on neuronal-expressed miRNAs, which predictably contributed to the evolution of human cognition (Hu et al. 2012). Figure 1 presents the layout of the study and the databases and algorithms on which it has been based. We utilized several well-established prediction algorithms of miRNA-binding sites that have shown satisfactory robustness in previous reports. We then combined these tools with regularly employed measures for genetic variation and conservation, to compare the genomes of 1,092 humans and 58 additional organisms, including the Neanderthal. Our findings demonstrate inverse correlation between the genomic variation around miRNA genes and their targets, with particularly pronounced differences in neuronal expressed genes.

Results

Genomic miRNA Sites Show Globally Higher Interspecies Conservation than Their Target Genes

To study the degree of conservation of miRNA genes, we analyzed 1,523 miRNA genomic sites downloaded from miRBase (version 17). These target a total of 2,685,771 miRNA-binding sites: 1,918,916 and 728,288 predicted sites derived from the DIANA-microT and the miRanda prediction algorithms, respectively, and 38,567 validated miRNA target sites of TarBase (version 6). The genomic coordinates for each of the TarBase validated miRNA-target gene pairs were identified using the microT prediction algorithm, because the TarBase database does not include such coordinates; finally, our enrichment analysis involved 24,364 protein-coding genes from the Ensembl Genome Browser.

To examine genomic conservation, we employed the microT and miRanda algorithms. Both of these algorithms do not depend on cross-species conservation (Miranda et al. 2006), which makes them suitable for such analyses. We first compared the conservational level of tested genomic sites with that of the baseline genomic conservation for each group of organisms, using the phyloP algorithm (Pollard et al. 2010). This analysis demonstrated consistently higher evolutionary conservation around the transcription start sites of miRNA genes compared with transcription start and end sites of protein-coding genes in primates, placental mammals, and vertebrates (Kolmogorov–Smirnov [KS] test, $P < 0.045$, $P < 0.042$, $P < 0.002$, respectively). Figure 2*a–c* presents these findings for predicted miRNA-binding sites and for validated binding sites derived from TarBase (see lists of organisms in each group in supplementary table S1, Supplementary Material online). The conserved region around miRNA sites was 0.4 kb, considerably narrower than the 1.0 kb around transcription start sites of protein-coding genes. This is compatible with the smaller genomic regions occupied by miRNAs. In contrast, sequences surrounding miRNA-binding sites in the target protein-coding genes were significantly less conserved than the 1 kb sequences around miRNAs and the start sites of protein-coding genes ($P < 0.001$, for all studied groups).

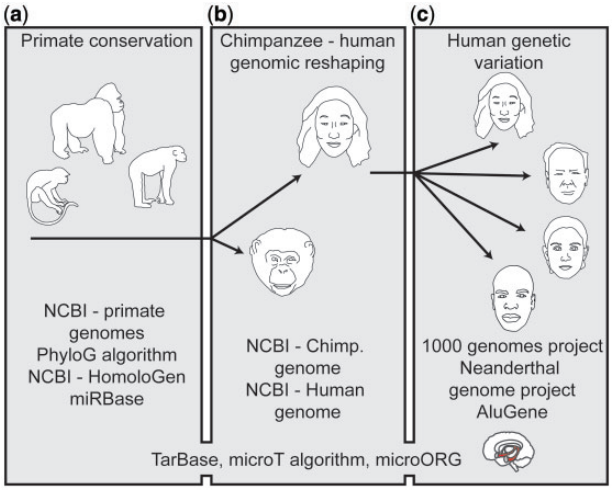

Fig. 1. Investigating miRNA evolution by complementary approaches and in different data sets. We predicted that miRNA regulation may be modulated by evolutionary processes in miRNA sites, miRNA-binding sites, or both, in an interlinked manner. To challenge this theory, we performed three lines of analyses. (*a*) The conservation of miRNA sites between primates was approached by examining primate genome sequences, downloaded from the National Center for Biotechnology Information (NCBI) database and miRBase and by implementing the phyloP algorithm. (*b*) Genomic reshaping processes of miRNA sites were studied by comparing the chimpanzee and human genomes. (*c*) Genomic variation between miRNA sites in diverse human populations was tested using the data sets from the 1000 Genomes project and the Neanderthal genome project. TarBase and MicroRNA.org and the microT algorithm were utilized at all levels and hippocampal-expressed transcripts (red marked brain structure, MicroRNA.org) served to focus on neuronal implications.

Global miRNA Sites Show Higher Human–Chimpanzee Genomic Alignments than Their Target Genes

To determine whether the higher conservation around primate miRNA genes was further subject to change at shorter evolutionary time scales, we compared genomic regions around miRNAs and protein-coding genes between the human and chimpanzee genomes. Pair-wise genomic alignments were downloaded from the University of California–Santa Cruz (UCSC) web site (http://hgdownload.soe.ucsc.edu/downloads.html, last accessed February 1, 2014). Aligning the hg19 and panTro3 assemblies by the BlastZ alignment program (Schwartz et al. 2003) (http://www.bx.psu.edu/miller_lab/, last accessed February 1, 2014) demonstrated high prospects for a successful alignment for regions surrounding miRNAs in the human and chimpanzee genomes. This alignment was higher than the parallel alignment of the transcription start and end sites of protein-coding genes. In comparison, both validated and predicted miRNA-binding

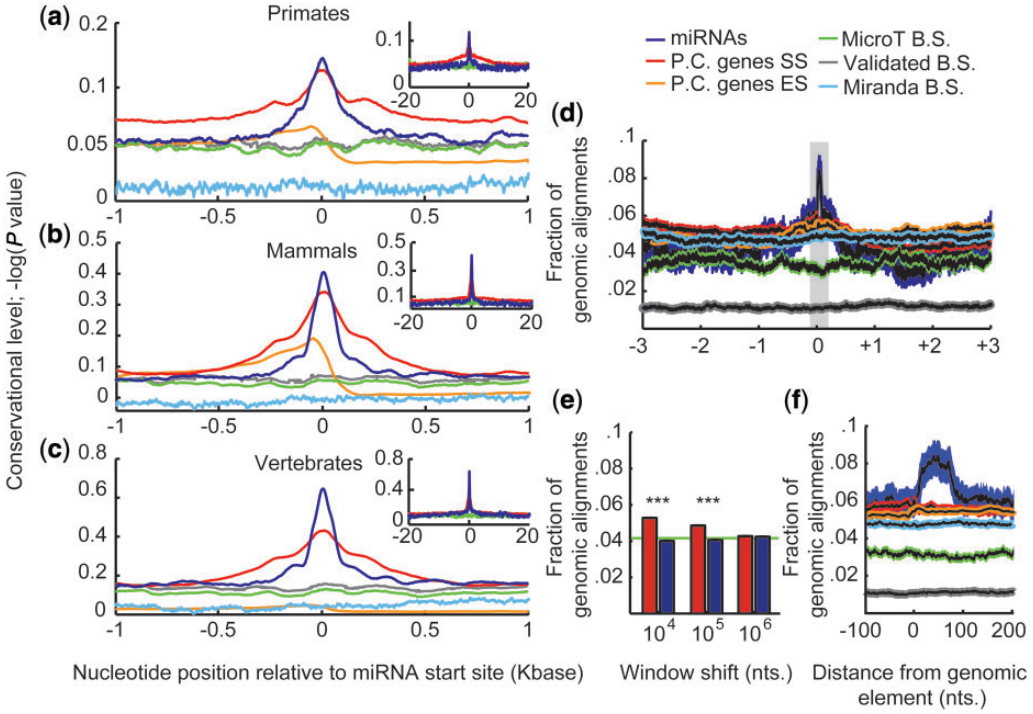

FIG. 2. High evolutionary conservation and increased genomic reshaping around primate miRNA transcription start sites. (*a*–*c*) PhyloP conservational levels as a function of genomic location, aligned across the transcription start site of miRNAs (dark blue), transcription start site of protein coding genes (P.C. genes SS; red), transcription end site of protein coding genes (P.C. genes ES; orange), and microT-predicated, validated, and miRanda-predicted miRNA-binding sites (green, gray, and light blue, correspondingly) for primates alone (*a*), placental mammals (*b*), and vertebrate mammals (*c*) (full list of organisms in supplementary table S2, Supplementary Material online). Color code shown in (*d*). Positive and negative values of the PhyloP conservational level indicate conserved sites and rapidly evolving regions, respectively. (*d*) Mean number of alignments between human and chimpanzee genomes as a function of physical distance in kilo nucleotides around several genomic elements. Color code as in (*a*). Note increased alignments around miRNA sites compared with other elements (KS test, $P < 0.0001$). Gray rectangle represents zoom-in region which is shown in (*f*). (*e*) Averaged level of alignments for windows of 10 K nucleotides long and a varying upstream shift from the genomic element start sites. Note the distinct differences between protein coding genes at distances of 10^4 and 10^5 (ANOVA and post hoc Tukey test, $P < 0.001$). (*f*) Zoom-in on the 400 nucleotides region represented by the gray rectangle in (*e*). The length of the region in which miRNA genomic alignment level differs from that of protein coding one is about 100 nucleotides.

sites in the protein-coding genes showed lower alignment (fig. 2*d*; KS test, $P < 0.0001$). The alignment around the different genomic elements equalized at a 1 Mb distance (fig. 2*e*), and the peak length for miRNA alignments was most prominent at 100 bases from the miRNAs transcription start site (fig. 2*f*), close to the average length of miRNAs in the genome.

Diverse Human Populations Show Low Genetic Variation within and near miRNA Genes

On the basis of our prediction of a unique role of miRNAs in the evolution of humans, we proceeded by comparing the levels of genetic variation around miRNA genes and other genomic elements between various human populations. For that purpose, we downloaded 1,092 sequenced human genomes from the 1000 genomes project (http://www.1000genomes.org/, last accessed March 14, 2014), which includes ethnic origin data. Single-nucleotide polymorphisms (SNPs) were studied in all human miRNAs. Mean allelic frequency (AF) values for these SNPs were then calculated in windows of 8 kb centered at the transcription start site of miRNA genes or their binding sites, corrected for the different degree of linkage disequilibrium (Nyholt 2004). We observed a sharp decrease in allele frequencies, suggesting strong conservation near miRNA transcription start sites for all four main human subpopulations (fig. 3*a*). The observed variation remained the same when excluding the mature miRNA sequences from the tested region (supplementary fig. S1, Supplementary Material online). Inversely, we quantified the averaged allele frequencies of SNPs in 1 kb windows (the length of the observed trough) centered around the miRNA-binding sites in both predicted and validated miRNA target genes. This analysis demonstrated larger variation than that observed for the regions surrounding transcription start sites of either miRNA or protein-coding genes (fig. 3*b*). The allelic frequencies of transcription end sites of protein-coding genes were similarly high as those of miRNA-binding sites. In comparison, other protein-coding genes and transcription start sites of the regulatory transcription factor genes showed lower and indistinguishable genomic variation (supplementary fig. S2 and table S2, Supplementary Material online), and noncoding regions in the genome displayed yet higher genomic variation than all of the other groups (fig. 3*b*). Also, intergenic miRNAs showed larger variation profiles compared with intragenic ones but

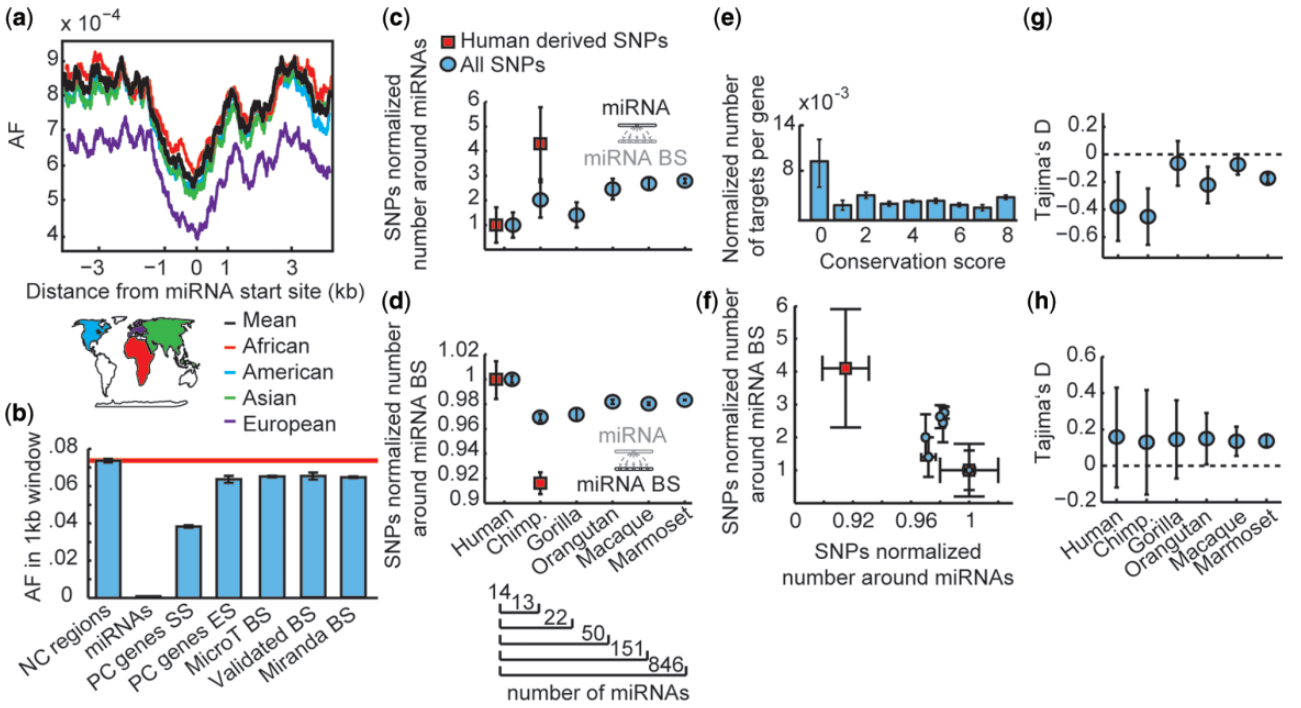

FIG. 3. Globally low genetic variation around miRNA sites. (*a*) Mean AF accounting for linkage disequilibrium as a function of physical distance in kb from the miRNA transcription start site, for four populations (African, American, Asian, and European) and their mean. All four populations display a 1,000 base trough, of similar depth, around miRNA sites. (*b*) Averaged AF in 20 kb windows of noncoding (NC) regions in the human genome; miRNA sites; transcription start and end sites of protein coding genes (PC genes SS and ES); and microT-predicted, validated, and miRanda-predicted miRNA-binding sites (miRNA BS). Horizontal red bar marks the noncoding regions (mean ± SEM, one-way ANOVA, $P < 0.001$). (*c*, *d*) Averaged normalized SNPs density around miRNA genes and miRNA-binding sites that are either unique to humans or conserved between humans and the noted organisms. MiRNA numbers are shown for each group. (*e*) Averaged number of microT-predicted miRNA-binding sites normalized by gene length, for genes with different conservation scores, "0" denoting human specific genes and "8" conservation all the way back to *Plasmodium falciparum* (one-way ANOVA, $P < 0.05$). (*f*) SNP density around miRNA (*X* axis) as a function of their binding sites (*Y* axis). Markers as in (*c*) and (*d*). (*g*, *h*) Averaged Tajima's *D* scores for miRNAs of different conservational levels (*g*) and their target sites (*h*). One-way ANOVA *P* values for miRNA effect < 0.05.

with far lower variation than protein-coding genes (supplementary fig. S3, Supplementary Material online).

Inverse SNP Densities around miRNA Genes and Their Binding Sites

Next, we wished to examine potential association between SNP densities around miRNAs and the parallel SNP densities around their target genes. To this end, we utilized the classification used by Hu et al. (2011) of the 1,523 known human miRNAs. MiRNAs were classified into those unique to humans, conserved between humans and Chimpanzee, common to humans, Chimpanzee, and Gorilla, or shared with all of those and Orangutan, Macaque, or Marmoset. Human-specific miRNA genes showed lower SNP density compared with miRNAs conserved in other primate species (fig. 3*c*, one-way analysis of variance [ANOVA] $P = 0.007$). Inversely, SNP densities around predicted binding sites of human-specific miRNAs were higher than those surrounding the binding sites of conserved miRNAs (fig. 3*d*, one-way ANOVA $P = 0.003$). Moreover, we found that the genetic diversity around miRNAs continued to increase throughout the evolution of the primate lineage, whereas the genetic diversity around their binding sites stopped declining in the common ancestor of human and chimpanzee. This is compatible with the evolutionary rates that were reported by others for miRNAs and their binding sites (Khaitovich et al. 2006; Lu et al. 2008; Meunier et al. 2013). To focus on events that occurred after the Human–Neanderthal split, we utilized data of the Neanderthal Genome project to classify human SNPs into those that are derived in humans (human specific) or ancestral in the Neanderthal (see Materials and Methods). Separation of the human and Neanderthal ancestral populations is estimated to have taken place 370,000 years ago (Noonan et al. 2006). Human-specific miRNA genes demonstrated yet lower SNPs density than those shared with the Neanderthal. Moreover, the target-binding sites of human-specific miRNAs showed higher SNPs density compared with other human SNPs (fig. 3*c* and *d*), supporting the prediction of favored new variants around target genes of human-specific miRNAs. The human-specific miRNAs comprise a relatively small group of 14 genes, yet this difference was statistically significant (one-way ANOVA $P = 0.012$ for miRNAs and 0.008 for miRNA-binding sites). Plotting SNP densities around miRNA-binding sites as a function of the mean SNP density around these miRNA genes highlighted these differences (fig. 3*f*). A similar effect, albeit somewhat less pronounced was observed for miRanda-predicted

Table 1. Nonredundant Cluster Enrichment Analysis of Targets of Human-Specific miRNAs.

Cluster	Annotation Groups in Cluster	Enrichment Score	Benjamini Corrected *P*
1	Pleckstrin homology (24/4), Pleckstrin homology type (22/3.4), regulation of Ras protein signal transduction (14/2.3)	3.33	0.03
2	Protein kinase C (11/1.8), diacylglycerol binding (10/1.6), lipid binding (18/2.4)	3.09	0.02
3	Cytoskeletal protein binding (33/5.4), actin binding (24/3.9), actin cytoskeleton (15/2.5)	2.99	0.01
4	Postsynaptic membrane (9/1.5), synapse (23/3.8), synapse part (18/2.9), cell junction (31/5.1)	2.51	0.05
5	Metal ion binding (166/27.1), cation binding (166/27.1), ion binding (168/27.5), zinc-finger (65/10.6)	2.09	0.015
6	Postsynaptic density (11/1.8), dendrite (11/1.8), cell soma (10/1.6), dendritic spine (4/4.5)	2.01	0.016
7	Cytoskeleton (61/10), microtubule cytoskeleton (61/8.4), nonmembrane-bounded organelle (90/14.7)	2	0.02

NOTE.—Seven clusters enriched with genes that are targets of human-specific miRNAs, with enrichment score larger than 2 (equivalent to *P* value = 0.01), are listed. For each annotation group, the numbers and percentage of involved genes are shown in the left and right side of the brackets, respectively. For each cluster, an enrichment score (−log 10 transform of the geometric mean of the *P* values of the gene groups from which the cluster is built) and the minimal Benjamini corrected *P* value of the specific gene groups in the cluster are shown.

miRNA-binding sites (supplementary fig. S4, Supplementary Material online). The inverse correlation between SNP densities in miRNA and miRNA-binding sites could not be evaluated for the TarBase-validated miRNA-binding sites, due to the small number of binding sites in each group.

Next, we predicted that the global evolutionary mechanisms that enabled SNP accumulation around binding sites for miRNAs would potentiate the capacity of these miRNAs to change gene regulation. In search for the timing of this process, we split the human genome into ancient genes conserved all the way back to *Plasmodium falciparum*, genes unique to *Homo sapiens*, and all other genes subclassified by their degree of conservation. We then calculated genomic conservation values between tested genes from these classified groups by using the HomoloGen conservation score (http://www.ncbi.nlm.nih.gov/, last accessed February 1, 2014). This analysis showed consistent evolutionary increases in the numbers of microT-predicted miRNA-binding sites per gene. Importantly, human-specific genes showed several-fold more miRNA-binding sites compared with the ancient and more conserved human genes (fig. 3*e*; see supplementary fig. S5, Supplementary Material online, for gene counts at each conservational level). A similar effect was seen for validated miRNA-binding sites (supplementary fig. S6, Supplementary Material online), suggesting that the speciation of hominids was accompanied by profound increase in the capacity of newly evolved miRNAs to regulate gene expression.

To examine the selection forces that underline these genetic diversity processes, we downloaded the Tajima's *D* test score as calculated for the 1000 Genomes project data set across the human genome (see Materials and Methods). Negative Tajima's *D* values signify an excess of low-frequency polymorphisms relative to expectation, indicating purifying selection. In comparison, positive Tajima's *D* values reflect low levels of both low- and high-frequency polymorphisms, indicating balancing selection. We observed lower Tajima's *D* values indicating purifying selection for miRNAs compared with protein coding genes and for both of these groups compared with the entire genome (KS test, *P* value < 0.01). This effect was observed across the entire population and separately for Utah Residents with Northern and Western European ancestry, Han Chinese in Beijing, China, and Yoruba Residents in Ibadan, Nigeria. We further observed lower Tajima's *D* values around miRNAs that are conserved at varying levels among primates (fig. 3*g*, one-way ANOVA *P* value < 0.05). No difference was observed for target sites of miRNAs of varying conservational levels (fig. 3*h*).

Targets of Human-Specific miRNAs Show Selectively Enriched Neuronal Functions

To determine whether targets of human-specific miRNAs are involved in any particular biological function, we performed nonredundant cluster analysis of enrichment using DAVID (http://david.abcc.ncifcrf.gov/home.jsp, last accessed February 1, 2014). The DAVID cluster analysis assembles gene groups with a high degree of overlap between them to single clusters. This offers a nonredundant procedure of gene enrichment analysis and showed no enrichment for the predicted target genes of nonhuman-specific miRNA conservation groups. In contrast, we did observe clear enrichment for the list of 624 genes that are predicted to be targets of one or more human-specific miRNAs (supplementary tables S5 and S6, Supplementary Material online). Thus, our analysis identified seven significantly enriched clusters at decreasing levels of enrichment scores, out of which the top two scores relate to global cellular signaling which takes place both in the brain and in other tissues (e.g., Ras protein signal transduction and protein kinase C), whereas the other five (clusters 3–7) associate with distinct neuronal functions. Benjamini corrected *P* values for these clusters highlight cytoskeletal elements ($P < 0.01$), metal ion binding ($P < 0.015$), and postsynaptic, dendritic, and somatic functions ($P < 0.016$) as most significant (table 1).

To approach the question of functional relevance of these findings, we examined miRNAs expressed both in the brain and in other tissues but at different levels. Specifically, we compared the 40 highest and 40 lowest expressed miRNAs in the hippocampus, a brain region for which miRNA

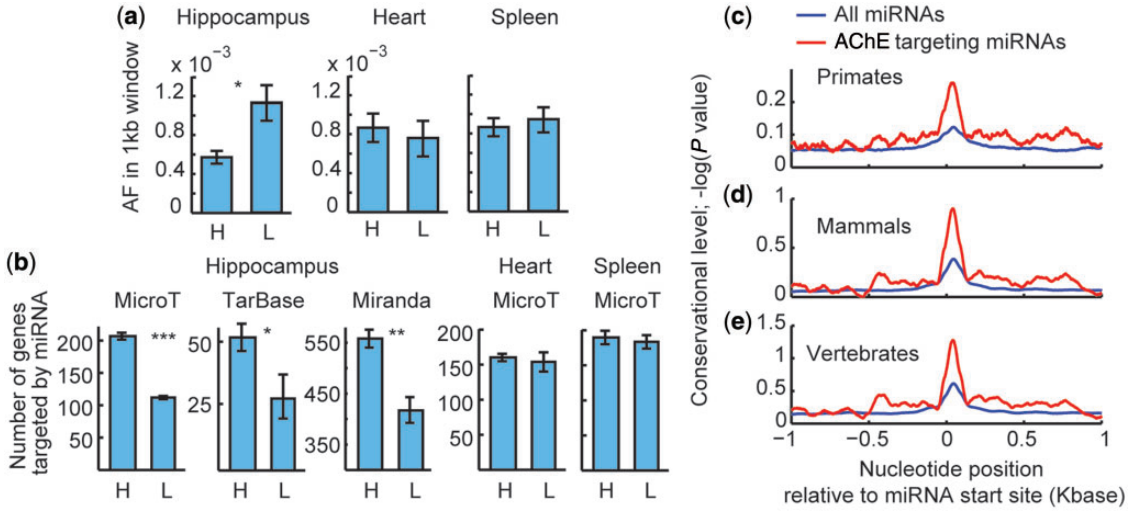

Fig. 4. Pronounced miRNA regulation in neuronal tissue. (*a*) Averaged AF sequences in 20 kb windows of Hippocampal, heart or spleen highly (H) and lowly (L) expressed miRNAs (*t*-test, $P < 0.05$). (*b*) Number of genes targeted by highly and lowly expressed hippocampal, heart or spleen miRNAs, based on MicroT-prediction algorithm, TarBase validated targets, or miRanda (in Hippocampus, *t*-test *P* value for microT < 0.001, for TarBase < 0.05, and for miRanda < 0.01). (*c*–*e*) PhyloP conservational levels as a function of genomic location, aligned across All miRNAs (blue) and ACHE-targeting miRNAs (red), for primates alone (*c*), placental mammals (*d*), and vertebrate mammals (*e*). *P* value ranges are marked by asterisks ($^*P < 0.05$, $^{**}P < 0.01$, and $^{***}P < 0.001$).

expression data were available, compared with other, nonneuronal tissues. Hu et al. (2012) show expression, albeit low, in the prefrontal cortex and cerebellum in humans of most of the human-specific miRNAs; however, none of the human-specific miRNAs were included in this group of selected hippocampal miRNAs, possibly because their low expression levels excluded them from our classification. The hippocampus is known to be involved in cognitive, navigation, and executive functions (van Strien et al. 2009). The top hippocampal-expressed miRNA genes showed significantly lower mean AF values than the bottom hippocampal-expressed miRNAs (fig. 4*a*; for lists of hippocampal miRNAs see supplementary table S3, Supplementary Material online), suggesting stronger selection against evolutionary accumulation of variations in regions surrounding brain-expressed miRNAs compared with other miRNA genes. Others proposed that miRNAs with more targets tend to be evolutionarily more stable than other miRNAs (Tang et al. 2010). Supporting and extending this prediction, microT-prediction analysis demonstrated that highly expressed human hippocampal miRNAs display lower genetic variation than the lowly expressed hippocampal miRNAs (fig. 4*a*) and target 2-fold more transcripts than the lowly expressed hippocampal miRNA genes (fig. 4*b*, $P < 0.001$). Increased targeting of Hippocampal miRNAs was also observed based on TarBase validated binding sites (fig. 4*b*, $P < 0.05$) and the miRanda prediction algorithm (fig. 4*b*, $P < 0.001$). In contrast, high and low expressed miRNAs in heart and spleen did not show such differences (fig. 4*a* and *b*). Also, groups of high and low hippocampal-expressed miRNAs bigger than 40 or smaller than 10 did not show this effect, suggesting that the increased targeting is limited to those miRNAs that show extremely high levels in the hippocampus and low levels elsewhere when compared with miRNAs showing low hippocampal levels. As a case test, we calculated the conservation scores of all of the miRNAs predicted to target the hippocampal-expressed acetylcholinesterase (*AChE*) gene (Berson et al. 2012; Shaltiel et al. 2013), which is also expressed in spleen cells albeit at considerably lower levels (Shaked et al. 2009). Both microT and miRanda analyses showed consistently higher conservation for *AChE*-targeted miRNAs compared with all other miRNAs for primates, placental mammals, and vertebrates (fig. 4*c*–*e*; KS test, $P < 0.05$, based on microT). This observation was also found based on the miRanda prediction algorithm (supplementary fig. S7, Supplementary Material online), consistent with the notion of high conservation of miRNAs targeting neuronal proteins.

To re-examine the functional relevance of our findings and exclude the possibility that a link between miRNAs and their targets would only hold true for nonvalidated miRNAs, we have next focused on two highly expressed, neuronal miRNAs with different conservation levels: the evolutionarily conserved miRNA-132 and the human-specific miRNA-941. The genomic site harboring miRNA-132 displayed high conservation scores across vertebrates, mammals, and primates, around a region of about 1.5 kb. In contradistinction, the genomic site harboring the three newly evolved copies of the human-specific miRNA-941 showed inert conservation scores, far lower than those of miRNA-132 in both mammals and primates (fig. 5*a*–*c*). Also, the binding sites of miRNA-132 have shown consistently lower conservational levels than those of miRNA-132 in vertebrates, mammals, and primates alike. In comparison, the binding sites of miRNA-941 occur at primate genomic regions with apparently higher conservation than that of the miRNA-941 gene itself (fig. 5*d*–*f*), such that the binding sites of these two miRNAs show inverse patterns to those of the miRNA genes.

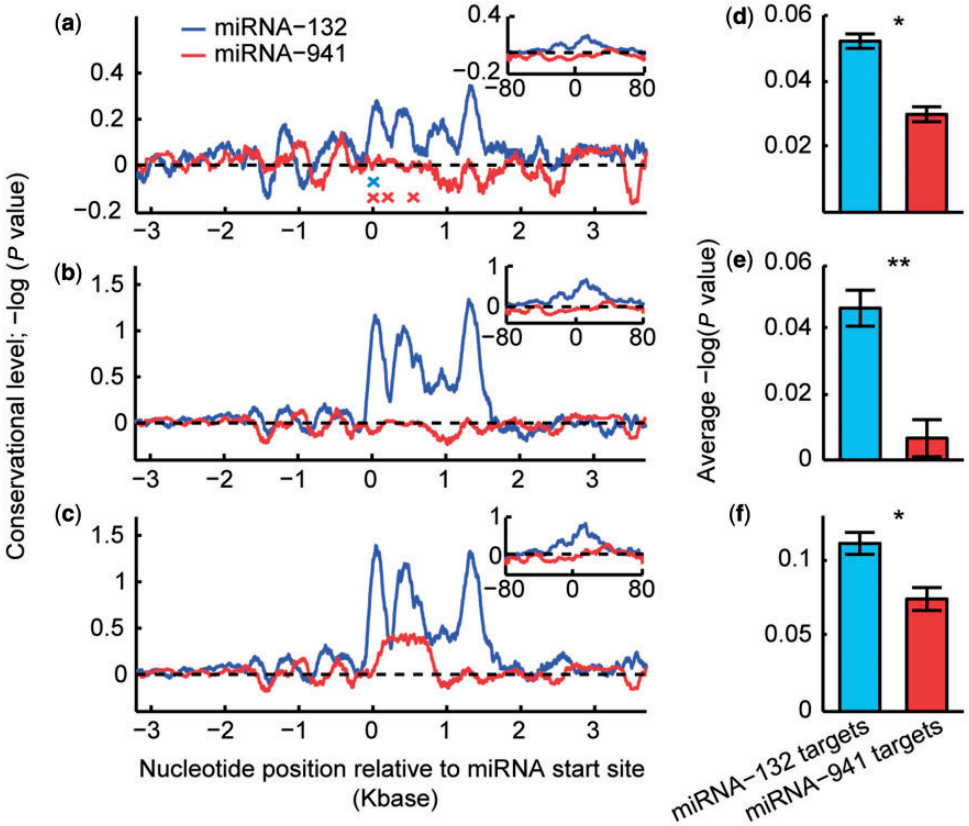

FIG. 5. Conservational levels around miR-132 and miR-941 inversely associate with the conservational levels of their targets. (*a*–*c*) Conservational levels around miR-132 (blue) and miR-941 (red) start sites as −log transformation of PhyloP-*P* values (see Materials and Methods). (*a*) Primates alone. (*b*) Placental mammals. (*c*) Vertebrate mammals. Crosses in (*a*) indicate miR-132 start site (blue) and miR-941 variants (red, miR-941-1, 2, and 4, in this order from left to right). Insets show wide genomic windows (*a*–*c*: from −80 to 80 kb). Graphs are smoothed with a 10% mean sliding window. (*d*–*f*) Averaged conservation levels for binding sites of miR-132 (blue) and miR-941 (red). (*d*) Primates alone (*t*-test, $P < 0.05$). (*e*) Placental mammals ($P < 0.01$). (*f*) Vertebrate mammals ($P < 0.05$). *P* value ranges are marked by asterisks ($^*P < 0.05$ and $^{**}P < 0.01$).

Discussion

By performing a detailed genomic dissection using a combination of computational approaches, we identified coevolution of miRNAs and their targets. Targets largely show globally inverse patterns of evolutionary changes than those of the miRNA genes. We found the great majority of miRNAs to be predictably more conserved during evolution than protein-coding genes, compatible with previous reports of purifying selection in some miRNA regions (Quach et al. 2009). Within all of the tested human subpopulations, we identified low levels of genomic variations and high levels of purifying selection around miRNA sequences that correlated with inversely high genomic diversity in their target sites. Furthermore, we found human-specific miRNAs to have more targets than conserved miRNAs, and their binding sites showed yet higher genomic diversity within diverse human populations than binding sites of conserved miRNAs.

The evolutionary conservation of miRNA genes and the inversely expedited evolution of miRNA-binding sites, from vertebrates through primates and in diverse human populations, are compatible with reports of rapid gain and loss of miRNA-binding sites over short evolutionary distances (Chen and Rajewsky 2007; Berezikov 2011). Also, several functional polymorphisms have been identified in miRNA-binding sites in humans (Abelson et al. 2005), but the sequences of mature miRNA genes hardly show such polymorphisms (Iwai and Naraba 2005). Genetic variation in target genes can influence their regulation by creating novel miRNA target sites but more likely by destroying existing ones, because any random mutation within an existing binding site may destroy it, but only specific mutations in a specific order will create a new binding site. Nevertheless, human-specific miRNAs have more binding sites, and those show greater diversity than the evolutionarily conserved miRNAs. This suggests that the recent- and possibly ongoing human evolution of novel miRNAs mainly operates by altering their binding sites in addition to creating new miRNA sites at loosely conserved genomic regions. Specifically, our findings suggest that early vertebrate evolution involved relatively moderate phenotypic outcome of changes in miRNAs and miRNA targets, overridden by other evolutionary processes occurring in these regions at that time. However, miRNA genes that emerged later than others show more binding sites compared with ancient ones, extending reports of robust miRNA regulation over mammalian genes (Friedman et al. 2009). This might further indicate that miRNA regulation reciprocally played a role in the phenotypic consequences of the selection process that

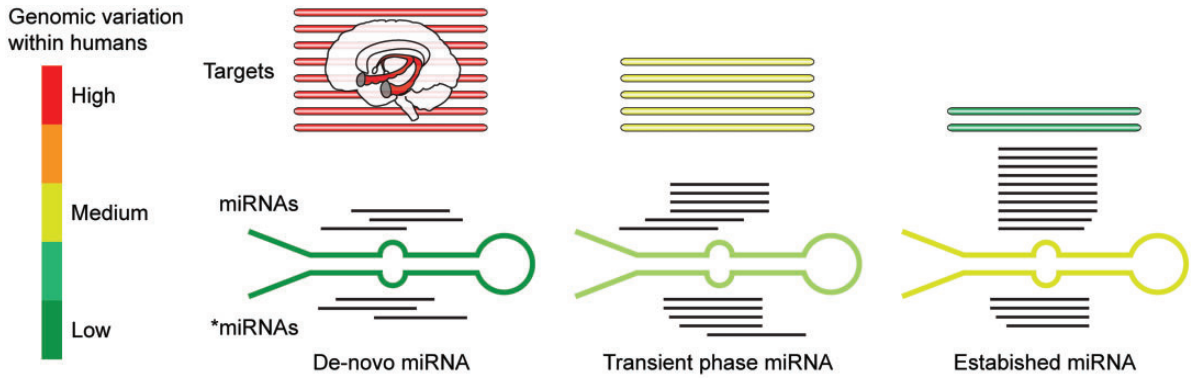

FIG. 6. Sequential evolution of de novo human miRNAs. Our model of the evolution of human miRNAs: de novo evolutionarily new, human-specific miRNAs (dark green) are expressed in low copy numbers (black lines) in both sequence direction (as miRNA or *miRNA) and arbitrarily interact with many targets (red lines), primarily brain-expressed ones. Transient phase miRNAs show increased expression levels and lower target numbers (yellow lines). Established miRNAs have already been subject to positive selection, which further reduces the number of targets per miRNA and aligns them along the miRNA (black lines). Pronounced selection against genomic variation in both the targets and the miRNA sequences maintains this state. The color code (left hand side) highlights these differences in genomic variation for both miRNAs and their targets (adapted from Chen and Rajewsky [2007] and Berezikov [2011]).

acted on these recently adopted target genes, such that genes that acquired numerous miRNA-binding sites were better suited for selection at a time when miRNA regulation had a profound phenotypic effect.

Strikingly, both previous studies and our analysis point at the evolution of miRNAs in humans as being dominated by three processes, which completely fit and extend the current model for new miRNA emergence. First, evolutionarily new, human-specific miRNAs are inserted at permissive genomic sites and are expressed in relatively low levels that increase gradually during the establishment of these novel miRNAs. Second, positive selection supports genomic variations within the binding sites acquired by the novel miRNAs. This is likely to reduce the number of targets per miRNA with evolutionary time. Finally, established miRNAs are expressed at high levels while being subject to strong selection against new variation in both the targets and the miRNA sequence. Figure 6 presents this model schematically.

Evolutionarily conserved neuronal miRNAs showed lowest levels of mean AF compared with other, nonneuronal miRNAs, suggesting prominent selection against modifications of brain-expressed miRNAs accompanied by ongoing evolutionary changes in their target sites. The association between genomic variation around neuronal human-specific miRNA genes and the corresponding miRNA-binding sites possibly points at an advantage conferred by the coordinated changes in these two genomic elements during human evolution. That the targets of the human-specific miRNAs mainly function in neuronal components and processes is compatible with changes in miRNA levels being involved in numerous neuronal disorders, for example, Alzheimer's and Parkinson's diseases (Hebert and De Strooper 2007; Barbash and Soreq 2012; Lau et al. 2013; Soreq et al. 2013). The notion that nervous tissues are subjected to tighter miRNA regulation than other tissues is also supported by the fact that neuronal expressed transcripts have longer 3′-UTR sequences, which are the main target region for miRNAs (Meunier et al. 2013). Furthermore, the association strength of coevolution becomes more robust when considering human-derived SNPs representing events that happened after the human–Neanderthal split, presumably, the epoch in which miRNA regulation had a notable phenotypic effect (Hu et al. 2012; Lu and Clark 2012). The yet higher association between SNP density around human-specific miRNAs and their targets might suggest increased phenotypic effect for miRNAs in humans during the epoch that followed the human–Neanderthal split. Although the group of human-specific miRNAs is composed of 14 miRNAs that are generally lowly expressed, they are likely to be physiologically functional in humans because they are localized to regions of low allelic diversity in the human genome and because their insertion into the human population is associated with larger genetic variation in their targets compared with other targets.

Taken together, our findings highlight the potentially important contribution of global coevolution of miRNAs and their binding sites along human speciation and call for future analyses and experimental tests to explore the contribution of specific miRNAs.

Materials and Methods

To address the possible evolutionary mechanisms that have shaped miRNA genes and their binding sites in target gene regions, we employed several sources of information and algorithms (code written in Matlab R2012a), as is briefly listed below.

Databases

The 1000 Genomes Project

This project includes low-coverage genotyping data of more than 1,092 individuals of known ethnic origins and was used to estimate genetic variation in specific genomic sites. (http://www.1000genomes.org/, last accessed March 14, 2014).

TarBase Version 6

Database of experimentally validated miRNA targets. This database includes about 65,000 experimental observations of miRNA regulation of target genes. It has a binary structure, such that a miRNA is reported to either regulate a gene or not regulate it. For each regulation, the experimental method that served to determine whether a regulation exists or not is given (http://diana.cslab.ece.ntua.gr/DianaToolsNew/index.php?r=tarbase, last accessed March 14, 2014).

Neanderthal Genome Project

The sequenced Neanderthal genome of a 38,000-year-old specimen from Vindija, Croatia (http://www.eva.mpg.de/neandertal/index.html, last accessed March 14, 2014).

National Center for Biotechnology Information HomoloGene Database

Information on homologous genes from organisms with sequenced genomes. HomoloGen was built by performing a BlastP analysis on protein sequences and mapping of the alignments back to their corresponding DNA sequences (http://www.ncbi.nlm.nih.gov/homologene/, last accessed March 14, 2014).

MiRBase Version 17

Includes miRNA annotations and sequences for organisms belonging to the primate lineage (http://www.mirbase.org/, last accessed March 14, 2014). Orthologs to human miRNAs were identified as in Hu et al. (2012).

MicroRNA.org—miRNA Expression Database

Includes information of miRNA expression from different tissues in different organisms (http://www.microrna.org/microrna/home.do, last accessed March 14, 2014).

Identifying Potential miRNA-Binding Sites

We used the "microT" algorithm of the DIANA lab (http://diana.cslab.ece.ntua.gr/, last accessed March 14, 2014) to identify predicted miRNA-binding sites. When defining a "miRNA binding site," one can use the validated miRNA-target database TarBase (http://diana.cslab.ece.ntua.gr/DianaToolsNew/index.php?r=tarbase, last accessed March 14, 2014) or implement an algorithm that identifies predicted miRNA-binding sites. The first option offers an added value in that each interrogated target has been experimentally validated. However, validated databases also unavoidably lag behind the field's development (TarBase6 only covers 871 miRNAs) and offer highly variable numbers of targets for different miRNAs (in TarBase6, 25% of the miRNAs have only one validated target, whereas 25% have more than 20 targets). Moreover, validated databases report whether the gene reacts to miRNA interference by an expression change, but they do not report specific binding sites in the gene or the number of binding sites for a given miRNA in a targeted gene. These limitations may partially reflect the embedded bias in miRNA research (the first seven significantly enriched with miRNA-regulated pathways in TarBase6 are prostate cancer, melanoma, long-term potentiation, acute myeloid leukemia, glioma, axon guidance, and renal cell carcinoma, including five cancers and two neuronal-related ones). However, miRNAs participate in many basic functional properties, and predicted binding sites for miRNAs have shown to be functional when considered globally (Hu et al. 2011) and to have a similar effect on human gene expression as validated binding sites (Lu and Clark 2012). Therefore, we set to delineate the general principles governing the coevolution of miRNA genes and their binding sites by utilizing a miRNA-binding site prediction approach, specifically the "microT" algorithm of the DIANA lab (http://diana.cslab.ece.ntua.gr/, last accessed March 14, 2014).

The MicroT Algorithm

The microT algorithm (DIANA lab) predicts miRNA-binding sites as described by Maragkakis et al. (2009). Briefly, the DIANA-microT 3.0 algorithm consists of 1) alignment of the miRNA sequence on the 3′-UTR of a protein coding gene, 2) identification of putative miRNA recognition elements (MREs) based on specific binding rules, 3) scoring of individual MREs according to their binding type and conservation profile, and 4) calculation of an overall miRNA target gene score through the weighted sum of all MRE scores lying on the 3′-UTR. The algorithm takes into account the known features of miRNA regulation, such as nucleotide composition flanking the binding sites or proximity of one binding site to another within the same 3′-UTR (Gaidatzis et al. 2007; Grimson et al. 2007).

Estimating AF

A marker **M** can have a series of alleles M_u, $u = 1, \ldots, k$. A sample of n individuals can therefore have several different genotypes at the locus, with n_{uv} copies of type M_u/M_v. The number n_u of copies of allele M_u can be found directly by summation: $n_u = 2n_{uu} + \sum_{v \neq u} n_{uv}$. The sample frequencies are $\tilde{P}_u = n_u/(2n)$ and $\tilde{P}_{uv} = n_{uv}/n$. The $\tilde{P}_{uv}$'s are unbiased maximum likelihood estimates of the population proportions P_{uv} (Cockerham 1973).

Human-Derived SNPs

Selective sweep scan or S SNPs were downloaded from UCSC. For these SNPs, the derived/ancestral states were determined in Neanderthal (Green et al. 2010). SNPs were defined as human derived if they appeared in at least four out of five present-day human genomes of diverse ancestry plus the human reference genome. All observed Neanderthal alleles were designated ancestral. The chimpanzee genome was used to determine the ancestral state. Because only one Neanderthal genome is available, polymorphic sites in humans may be present in Neanderthal as well. It could be that for many of those sites, the human and Neanderthal are derived relative to chimpanzee, yet the effect in figure 3*c* and *d* points at an enrichment of truly human-derived SNPs within the subset of SNP that were identified as human derived.

The PhyloP Algorithm

This algorithm calculates conservation or acceleration *P* values based on an alignment and a model of neutral evolution by computing a null distribution for the total number of substitutions from the tree model, an estimate of the number of substitutions that have actually occurred. The *P* value of this estimate is the null distribution. The method is

based on a phylogenetic hidden Markov model and does not require element boundaries to be determined a priori, making it particularly useful for identifying noncoding sequences (http://compgen.bscb.cornell.edu/phast/, last accessed March 14, 2014).

Pair-Wise Genomic Alignments of Human and Chimpanzee

Pairwise genomic alignments were downloaded from the UCSC web site (http://hgdownload.soe.ucsc.edu/downloads.html, last accessed March 14, 2014). The hg19 and panTro3 assemblies were aligned by the BlastZ alignment program(Schwartz et al. 2003) (http://www.bx.psu.edu/miller_lab/, last accessed March 14, 2014). BlastZ is an independent, modified implementation of the Gapped Blast algorithm (Altschul et al. 1997) specifically designed for aligning two long genomic sequences, both to attain efficiency adequate for aligning entire mammalian genomes and to increase its sensitivity. The BlastZ scoring matrix (Q parameter) used is brought as supplementary table S4, Supplementary Material online.

Tajima's *D* Score

The human genome was fractionated to windows of 30 kb (Pybus et al. 2014), and for each window, the Tajima's *D* score (Tajima 1989) was calculated across the genomes existing in the 1000 Genomes project. Briefly, the Tajima's *D* score is a normalized version of $\pi - \Theta$, when π is the observed average pairwise difference and Θ is the expected average pairwise difference assuming a neutral population with mutational drift.

Supplementary Material

Supplementary figures S1–S7 and table S1–S6 are available at *Molecular Biology and Evolution* online (http://www.mbe.oxfordjournals.org/).

Acknowledgments

The authors are grateful to Dr Karl Skorecki, Haifa, for fruitful discussions. This work was supported by the European Research Council Advanced Award 321501 to H.S. S.B. is an incumbent of the TEVA National Network of Excellence in Neuroscience—NNE fellowship.

References

Abelson JF, Kwan KY, O'Roak BJ, Baek DY, Stillman AA, Morgan TM, Mathews CA, Pauls DL, Rasin MR, Gunel M, et al. 2005. Sequence variants in SLITRK1 are associated with Tourette's syndrome. *Science* 310:317–320.

Altschul SF, Madden TL, Schaffer AA, Zhang J, Zhang Z, Miller W, Lipman DJ. 1997. Gapped BLAST and PSI-BLAST: a new generation of protein database search programs. *Nucleic Acids Res.* 25:3389–3402.

Ambros V. 2003. MicroRNA pathways in flies and worms: growth, death, fat, stress, and timing. *Cell* 113:673–676.

Babbitt CC, Fedrigo O, Pfefferle AD, Boyle AP, Horvath JE, Furey TS, Wray GA. 2010. Both noncoding and protein-coding RNAs contribute to gene expression evolution in the primate brain. *Genome Biol Evol.* 2:67–79.

Bagga S, Bracht J, Hunter S, Massirer K, Holtz J, Eachus R, Pasquinelli AE. 2005. Regulation by let-7 and lin-4 miRNAs results in target mRNA degradation. *Cell* 122:553–563.

Barbash S, Soreq H. 2012. Threshold-independent meta-analysis of Alzheimer's disease transcriptomes shows progressive changes in hippocampal functions, epigenetics and microRNA regulation. *Curr Alzheimer Res.* 9:425–435.

Berezikov E. 2011. Evolution of microRNA diversity and regulation in animals. *Nat Rev Genet.* 12:846–860.

Berson A, Barbash S, Shaltiel G, Goll Y, Hanin G, Greenberg DS, Ketzef M, Becker AJ, Friedman A, Soreq H. 2012. Cholinergic-associated loss of hnRNP-A/B in Alzheimer's disease impairs cortical splicing and cognitive function in mice. *EMBO Mol Med.* 4:730–742.

Chen K, Rajewsky N. 2007. The evolution of gene regulation by transcription factors and microRNAs. *Nat Rev Genet.* 8(2):93–103.

Cockerham CC. 1973. Analyses of gene frequencies. *Genetics* 74:679–700.

Enright AJ, John B, Gaul U, Tuschl T, Sander C, Marks DS. 2003. MicroRNA targets in *Drosophila*. *Genome Biol.* 5:R1.

Fineberg SK, Kosik KS, Davidson BL. 2009. MicroRNAs potentiate neural development. *Neuron* 64:303–309.

Friedman RC, Farh KK, Burge CB, Bartel DP. 2009. Most mammalian mRNAs are conserved targets of microRNAs. *Genome Res.* 19:92–105.

Gaidatzis D, van Nimwegen E, Hausser J, Zavolan M. 2007. Inference of miRNA targets using evolutionary conservation and pathway analysis. *BMC Bioinformatics* 8:69.

Green RE, Krause J, Briggs AW, Maricic T, Stenzel U, Kircher M, Patterson N, Li H, Zhai W, Fritz MH, et al. 2010. A draft sequence of the Neandertal genome. *Science* 328:710–722.

Grimson A, Farh KK, Johnston WK, Garrett-Engele P, Lim LP, Bartel DP. 2007. MicroRNA targeting specificity in mammals: determinants beyond seed pairing. *Mol Cell* 27:91–105.

He L, Hannon GJ. 2004. MicroRNAs: small RNAs with a big role in gene regulation. *Nat Rev Genet.* 5:522–531.

Hebert SS, De Strooper B. 2007. Molecular biology. miRNAs in neurodegeneration. *Science* 317:1179–1180.

Hu HY, Guo S, Xi J, Yan Z, Fu N, Zhang X, Menzel C, Liang H, Yang H, Zhao M, et al. 2011. MicroRNA expression and regulation in human, chimpanzee, and macaque brains. *PLoS Genet.* 7:e1002327.

Hu HY, He L, Fominykh K, Yan Z, Guo S, Zhang X, Taylor MS, Tang L, Li J, Liu J, et al. 2012. Evolution of the human-specific microRNA miR-941. *Nat Commun.* 3:1145.

Iwai N, Naraba H. 2005. Polymorphisms in human pre-miRNAs. *Biochem Biophys Res Commun.* 331:1439–1444.

Khaitovich P, Enard W, Lachmann M, Paabo S. 2006. Evolution of primate gene expression. *Nat Rev Genet.* 7:693–702.

King MC, Wilson AC. 1975. Evolution at two levels in humans and chimpanzees. *Science* 188:107–116.

Konopka G, Friedrich T, Davis-Turak J, Winden K, Oldham MC, Gao F, Chen L, Wang GZ, Luo R, Preuss TM, et al. 2012. Human-specific transcriptional networks in the brain. *Neuron* 75:601–617.

Liang H, Li WH. 2009. Lowly expressed human microRNA genes evolve rapidly. *Mol Biol Evol.* 26:1195–1198.

Lau P, Bossers K, Janky R, Salta E, Frigerio CS, Barbash S, Rothman R, Sierksma ASR, Thathiah A, Greenberg D, et al. 2013. Alteration of the microRNA network during the progression of Alzheimer's disease. *EMBO Mol Med.* 5(10):1613–1634.

Lu J, Clark AG. 2012. Impact of microRNA regulation on variation in human gene expression. *Genome Res.* 22:1243–1254.

Lu J, Shen Y, Wu Q, Kumar S, He B, Shi S, Carthew RW, Wang SM, Wu CI. 2008. The birth and death of microRNA genes in *Drosophila*. *Nat Genet.* 40:351–355.

Maragkakis M, Alexiou P, Papadopoulos GL, Reczko M, Dalamagas T, Giannopoulos G, Goumas G, Koukis E, Kourtis K, Simossis VA, et al. 2009. Accurate microRNA target prediction correlates with protein repression levels. *BMC Bioinformatics* 10:295.

Meunier J, Lemoine F, Soumillon M, Liechti A, Weier M, Guschanski K, Hu H, Khaitovich P, Kaessmann H. 2013. Birth and expression evolution of mammalian microRNA genes. *Genome Res.* 23:34–45.

Miranda KC, Huynh T, Tay Y, Ang YS, Tam WL, Thomson AM, Lim B, Rigoutsos I. 2006. A pattern-based method for the identification of

MicroRNA binding sites and their corresponding heteroduplexes. *Cell* 126:1203–1217.

Noonan JP, Coop G, Kudaravalli S, Smith D, Krause J, Alessi J, Chen F, Platt D, Paabo S, Pritchard JK, et al. 2006. Sequencing and analysis of Neanderthal genomic DNA. *Science* 314:1113–1118.

Nowick K, Gernat T, Almaas E, Stubbs L. 2009. Differences in human and chimpanzee gene expression patterns define an evolving network of transcription factors in brain. *Proc Natl Acad Sci U S A.* 106: 22358–22363.

Nyholt DR. 2004. A simple correction for multiple testing for single-nucleotide polymorphisms in linkage disequilibrium with each other. *Am J Hum Genet.* 74:765–769.

Oldham MC, Horvath S, Geschwind DH. 2006. Conservation and evolution of gene coexpression networks in human and chimpanzee brains. *Proc Natl Acad Sci U S A.* 103:17973–17978.

Olsen PH, Ambros V. 1999. The lin-4 regulatory RNA controls developmental timing in *Caenorhabditis elegans* by blocking LIN-14 protein synthesis after the initiation of translation. *Dev Biol.* 216:671–680.

Pollard KS, Hubisz MJ, Rosenbloom KR, Siepel A. 2010. Detection of nonneutral substitution rates on mammalian phylogenies. *Genome Res.* 20:110–121.

Pybus M, Dall'olio GM, Luisi P, Uzkudun M, Carreno-Torres A, Pavlidis P, Laayouni H, Bertranpetit J, Engelken J. 2014. 1000 Genomes Selection Browser 1.0: a genome browser dedicated to signatures of natural selection in modern humans. *Nucleic Acids Res.* 42(Database issue):D903–D909.

Quach H, Barreiro LB, Laval G, Zidane N, Patin E, Kidd KK, Kidd JR, Bouchier C, Veuille M, Antoniewski C, et al. 2009. Signatures of purifying and local positive selection in human miRNAs. *Am J Hum Genet.* 84:316–327.

Roux J, Gonzalez-Porta M, Robinson-Rechavi M. 2012. Comparative analysis of human and mouse expression data illuminates tissue-specific evolutionary patterns of miRNAs. *Nucleic Acids Res.* 40:5890–5900.

Schwartz S, Kent WJ, Smit A, Zhang Z, Baertsch R, Hardison RC, Haussler D, Miller W. 2003. Human-mouse alignments with BLASTZ. *Genome Res.* 13:103–107.

Shaked I, Meerson A, Wolf Y, Avni R, Greenberg D, Gilboa-Geffen A, Soreq H. 2009. MicroRNA-132 potentiates cholinergic anti-inflammatory signaling by targeting acetylcholinesterase. *Immunity* 31: 965–973.

Shaltiel G, Hanan M, Wolf Y, Barbash S, Kovalev E, Shoham S, Soreq H. 2013. Hippocampal microRNA-132 mediates stress-inducible cognitive deficits through its acetylcholinesterase target. *Brain Struct Funct.* 218:59–72.

Somel M, Liu X, Tang L, Yan Z, Hu H, Guo S, Jiang X, Zhang X, Xu G, Xie G, et al. 2011. MicroRNA-driven developmental remodeling in the brain distinguishes humans from other primates. *PLoS Biol.* 9: e1001214.

Soreq L, Salomonis N, Bronstein M, Greenberg DS, Israel Z, Bergman H, Soreq H. 2013. Small RNA sequencing-microarray analyses in Parkinson leukocytes reveal deep brain stimulation-induced splicing changes that classify brain region transcriptomes. *Front Mol Neurosci.* 6:10.

Stark A, Brennecke J, Russell RB, Cohen SM. 2003. Identification of *Drosophila* microRNA targets. *PLoS Biol.* 1:E60.

Tajima F. 1989. Statistical method for testing the neutral mutation hypothesis by DNA polymorphism. *Genetics* 123:585–595.

Tang T, Kumar S, Shen Y, Lu J, Wu ML, Shi S, Li WH, Wu CI. 2010. Adverse interactions between micro-RNAs and target genes from different species. *Proc Natl Acad Sci U S A.* 107:12935–12940.

van Strien NM, Cappaert NL, Witter MP. 2009. The anatomy of memory: an interactive overview of the parahippocampal-hippocampal network. *Nat Rev Neurosci.* 10:272–282.